Moss, J., & Vaughan, M. (1977) *J. Biol. Chem. 252*, 2455–2457.

Moss, J., & Richardson, S. H. (1978) *J. Clin. Invest. 62*, 281–285.

Moss, J., & Vaughan, M. (1978) *Proc. Natl. Acad. Sci. U.S.A. 75*, 3621–3624.

Moss, J., & Stanley, S. J. (1981) *Proc. Natl. Acad. Sci. U.S.A. 78*, 4809–4812.

Moss, J., & Vaughan, M. (1981) *Mol. Cell. Biochem. 37*, 75–90.

Moss, J., Manganiello, V. C., & Vaughan, M. (1976) *Proc. Natl. Acad. Sci. U.S.A. 73*, 4424–4427.

Moss, J., Garrison, S., Oppenheimer, N. J., & Richardson, S. H. (1979a) *J. Biol. Chem. 254*, 6270–6272.

Moss, J., Stanley, S. J., & Oppenheimer, N. J. (1979b) *J. Biol. Chem. 254*, 8891–8894.

Moss, J., Stanley, S. J., & Watkins, P. A. (1980) *J. Biol. Chem. 255*, 5838–5840.

Moss, J., Stanley, S. J., Burns, D. L., Hsia, J. A., Yost, D. A., Myers, G. A., & Hewlett, E. L. (1983) *J. Biol. Chem. 258*, 11879–11882.

Ogata, N., Ueda, K., & Hayaishi, O. (1980a) *J. Biol. Chem. 255*, 7610–7615.

Ogata, N., Ueda, K., Kagamiyama, H., & Hayaishi, O. (1980b) *J. Biol. Chem. 255*, 7616–7620.

Oppenheimer, N. J. (1978) *J. Biol. Chem. 253*, 4907–4910.

Oppenheimer, N. J., & Bodley, J. W. (1981) *J. Biol. Chem. 256*, 8579–8581.

Pappenheimer, A. M., Jr. (1977) *Annu. Rev. Biochem. 46*, 69–94.

Pekala, P. H., & Moss, J. (1983) *Curr. Top. Cell. Regul. 22*, 1–49.

Riquelme, P. T., Burzio, L. O., & Koide, S. S. (1979) *J. Biol. Chem. 254*, 3018–3028.

Segel, J. H. (1975) *Enzyme Kinetics*, pp 273–330, Wiley, New York.

Ueda, K., Okayama, H., Fukushima, M., & Hayaishi, O. (1975) *J. Biochem. (Tokyo) 77*, 1p.

Van Ness, B. G., Howard, J. B., & Bodley, J. W. (1980a) *J. Biol. Chem. 255*, 10710–10716.

Van Ness, B. G., Howard, J. B., & Bodley, J. W. (1980b) *J. Biol. Chem. 255*, 10717–10720.

Vaughan, M., & Moss, J. (1981) *Curr. Top. Cell. Regul. 20*, 205–246.

Watkins, P. A., Moss, J., & Vaughan, M. (1981) *J. Biol. Chem. 256*, 4895–4899.

Small-Angle Neutron Scattering Study of Lateral Phase Separation in Dimyristoylphosphatidylcholine–Cholesterol Mixed Membranes†

W. Knoll,* G. Schmidt, K. Ibel,‡ and E. Sackmann

Physik Department E22, Biophysics Group, Technical University of Munich, D-8046 Garching, FRG

Received December 26, 1984

ABSTRACT: The small-angle neutron scattering (SANS) technique developed previously is used to study the lateral phase separation in dimyristoylphosphatidylcholine (DMPC)–cholesterol mixed vesicles in the L_α (35 °C) and $L_{\beta'}$ (7 °C) phase of DMPC. To increase the sensitivity of the previous method, we apply the so-called inverse contrast variation technique where contrast matching is performed at a constant H_2O/D_2O ratio by varying the ratio of DMPC with deuterated and protonated hydrocarbon chains. Phase boundaries can be determined to an accuracy of ±0.5 mol %. In parallel experiments phase separation in the $L_{\beta'}$ phase was also studied by freeze–fracture electron microscopy. For DMPC in the L_α phase complete miscibility is clearly established up to cholesterol molar fractions of $x_c = 0.14$. Strong evidence is provided that this is also the case up to $x_c \approx 0.45$. Cholesterol is no longer soluble above this limit and precipitates as small crystallites. For the $L_{\beta'}$ phase (7 °C) phase boundaries are clearly established at $x_{c1} = 0.08$ and $x_{c2} = 0.24$, and very strong evidence is provided for two additional boundaries at $x_{c3} = 0.435$ and $x_{c4} \approx 1.0$. At $0 \leq x_c \leq x_{c1}$ the mixture forms a tilted solid solution in both the $L_{\beta'}$ and $P_{\beta'}$ phase while at $x_{c1} \leq x_c \leq x_{c2}$ this phase coexists with a nontilted mixture containing 24 mol % cholesterol. At $x_{c2} \leq x_c \leq x_{c3}$ a second region exists where mixtures containing 24 and 43.5 mol % cholesterol coexist within the plane of the membrane. To fulfill the phase rule, x_{c2} must correspond to a stoichiometric mixture which would reconcile the concepts of phase separation and complex formation. Our freeze–fracture studies do not provide evidence for a decrease of the repeat distance of the ripple phase at $x_c \leq 0.08$ and for a regular ripple phase with defined ripple distance within the first coexistence region.

Since cholesterol is a major component of plasma membranes, its interaction with phospholipids in particular synthetic lecithins has been studied extensively in bilayers and monolayers (Albrecht et al., 1981; Cadenhead & Müller-Landau, 1984). A variety of methods has been applied including calorimetry (Mabrey et al., 1978; Estep et al., 1978), densitometry (Melchior et al., 1980), X-ray or electron diffraction (Hui & He, 1983), and spectroscopic techniques (Recktenwald & McConnell, 1981).

Despite this wealth of experimental data the thermodynamic and structural properties of the cholesterol–lecithin mixture

---

† This work was supported by the Bundesministerium für Forschung und Technologie.

‡ Permanent address: Institut Laue-Langevin, 156 X Centre de Tri, F-38042 Grenoble Cedex, France.

0006-2960/85/0424-5240$01.50/0

is far from being understood. Most workers come to the conclusion that this mixture exhibits immiscibility if the lecithin is in the crystalline ($P_{\beta'}$ or $L_{\beta'}$) state both in bilayers and in monolayers. On the basis of spectroscopic studies it has also been postulated that at low cholesterol contents lateral phase separation occurs in the L_α phase of DMPC (Recktenwald & McConnell, 1981). However, there are also numerous attempts to interpret the experimental data in terms of the formation of stoichiometric complexes with cholesterol to phospholipid ratios of 1:21, 1:7, and 1:3 (Cadenhead & Müller-Landau, 1984; Gershfield, 1978). A major problem is to distinguish between lateral phase separation and a decomposition of the lipid mixture into vesicles of different composition. This problem can be overcome by combining the spectroscopic or calorimetric measurements with morphological studies such as freeze-fracture electron microscopy (EM)[1] (Gebhardt et al., 1977; Copland & McConnell, 1980). Another problem is that fluid-fluid or solid-solid immiscibility can hardly be detected by calorimetric and spectroscopic techniques. Thus, molecular motions such as lateral diffusion depend on the lipids packing density (Galla et al., 1979), and a nonideal behavior of the molar volume of a fluid mixture can be erroneously taken as lateral phase separation. In order to overcome the second problem, we introduced the small-angle neutron scattering in combination with the contrast variation technique as a tool to establish phase diagrams of lipid mixtures (Knoll et al., 1981a). This technique makes use of the very large difference of the scattering cross sections of deuterated and protonated hydrocarbons and is thus well suited to detect heterogeneities of lipid distributions (Knoll et al., 1981b).

In the present work we apply the SANS technique in order to study the problem of phase separation in the DMPC-cholesterol mixture above (T = 35 °C) and well below (T = 7 °C) the chain melting transition temperature of the lecithin. Two contrast variation techniques are applied: the conventional technique and the inverse contrast variation method (Knoll et al., 1985a) which will be denoted as ICV in the following. The ICV technique enables a better correction of the incoherent neutron scattering and is much more sensitive against phase instabilities than is the conventional method. Thus, the compositions of phase boundaries may be determined to an accuracy of ±0.5%. In fact, the technique had to be introduced in order to study the cholesterol-DMPC mixture since it turned out that the conventional technique is not sensitive enough for this system. With this technique, phase boundaries are observed at 8, 24, and 43.5 mol % cholesterol for the $L_{\beta'}$ phase of DMPC while in the L_α phase a phase boundary was detected at 43.5%.

In a parallel experiment we restudied the mixed vesicles with the freeze-fracture technique at the compositions of the phase boundaries.

MATERIALS AND METHODS

1,2-Dimyristoyl-*sn*-glycero-3-phosphocholine (DMPC) was obtained from Fluka (Buchs, Switzerland). The same compound with deuterated fatty acid chains (DMPC-d_{54}) was from Avanti (Birmingham, AL) and cholesterol was from Serva (Heidelberg, Germany). All lipids gave a single spot on thin-layer chromatography and were used without further purification. The DMPC-d_{54} exhibits the chain melting transition at T_m = 18.7 °C and the pretransition at T_p = 13.0 °C. Thin-walled liposomes were prepared as described previously (Knoll et al., 1981a) by the solvent deposition technique. The H_2O/D_2O ratio of the water mixtures was controlled by densitometry and neutron transmission measurements (Knoll et al., 1985b). For the inverse contrast variation technique, the ratio of deuterated to nondeuterated DMPC was adjusted by mixing the two components in appropriate ratios. The liposomes were freshly prepared at most 2 h before each measurement. The total lipid concentration was 10^{-2} M.

The SANS experiments were performed with the D11 camera at the Institute Laue-Langevin (Grenoble, France). The samples were contained in a $1 \times 2 \times 0.1$ cm^3 quartz cuvette which was situated in a thermostated sample holder the temperature of which was controlled to ±0.5 °C. The neutron wavelength was λ = 10 Å, and the range of momentum transfer was $0.23 \times 10^{-2} < \kappa < 2.2 \times 10^{-2}$ A^{-1}. The scattered neutron flux was recorded within 10-20 min depending on the contrast.

The samples for the freeze-fracture study were prepared in the usual way by rapid freezing of vesicle suspensions sandwiched between two gold plates. The frozen samples were fractured in a Balzers (BAF 400) freeze-fracture device. Pt shadowing was performed under an angle of incidence of 45°. The micrographs were taken in a Philips (EM 400 T) electron microscope.

The low-angle scattering curves were analyzed as previously (Knoll et al., 1981a) in terms of the Kratky-Porod model of two-dimensional systems according to which the low-angle scattering intensity at the scattering vector, κ, is related to the thickness of gyration, R_d, of the lipid lamellas as

$$I(\kappa)\kappa^2 = I_0 \exp[-R_d{}^2\kappa^2] \quad (1)$$

The essential quantity in the present context is the scattering intensity, I_0, at zero scattering angle which is a function of the average contrast between the lipid layer and the aqueous phase and contains all the information concerning phase separation (Knoll et al., 1981a). For the slightly sonicated vesicle preparation the Kratky-Porod law is well fulfilled at scattering angles above $\kappa > 1 \times 10^{-2}$ Å^{-1} (cf. Figure 1), and I_0 may therefore be determined by extrapolation.

For the following brief summary of the contrast variation technique consider a binary mixture of DMPC and cholesterol with an initial molar fraction x_c of the latter and assume that it decomposes into two phases, 1 and 2, with cholesterol molar fractions x_1 and x_2, respectively. I_0 is then given by (Knoll et al., 1981b)

$$I_0 \propto \frac{x_2 - x_c}{x_2 - x_1}(\bar{\rho}_1 - \rho_s)^2 + \frac{x_c - x_1}{x_2 - x_1}(\bar{\rho}_2 - \rho_s)^2 \quad (2)$$

where ρ_s is the so-called scattering length density of the H_2O/D_2O mixture and where $\bar{\rho}_1$ and $\bar{\rho}_2$ are the average scattering length densities of the two phases. In the conventional technique the DMPC is deuterated, and I_0 is measured as a function of the D_2O content (or ρ_s) of the aqueous phase. The phase boundaries may be determined from plots of I_0 vs. the D_2O content of the aqueous phase if $\bar{\rho}_1$, $\bar{\rho}_2$, and ρ_s are measured separately by densitometry (Schmidt & Knoll, 1985).

In the inverse contrast technique the H_2O/D_2O ratio (or ρ_s) is kept constant while $\bar{\rho}_1$ and $\bar{\rho}_2$ are varied by replacing the DMPC-d_{54} by a mixture of the deuterated and the nondeuterated compound. I_0 is now measured as a function of the molar fraction x of the deuterated lecithin. As shown pre-

---

[1] Abbreviations: DMPC, dimyristoylphosphatidylcholine; DSPC, distearoylphosphatidylcholine; DMPC-d_{54}, dimyristoylphosphatidylcholine with perdeuterated chains; SANS, small-angle neutron scattering; ICV, inverse contrast variation; EM, electron microscopy; TEMPO, 2,2,6,6-tetramethylpiperidinyl-1-oxy.

Table I: Summary of Scattering Lengths, b, and Molecular Volumes, V, of Lipid Molecules and of Phase Boundaries

	$T = 7$ °C	$T = 35$ °C	$b_i/10^{-12}$ cm	remarks
DMPC	$V = 1024$ Å^3	$V = 1099$ Å^3	$b_D{}^P = 3.101$	$T_p = 13.5$ °C; $T_m = 23.8$ °C
DMPC-d_{54}	$V = 1025$ Å^3	$V = 1093$ Å^3	$b_D{}^d = 53.83^a$	$T_p = 13.0$ °C; $T_m = 18.7$ °C
cholesterol	$V = 628$ Å$^{3\,b}$	$V = 629$ Å$^{3\,b}$	$b_C = 1.325$	
phase boundaries	$x_{c1} = 0.08$; $V_1 = 975$ Å^3 $x_{c2} = 0.24$; $V_2 = 925$ Å^3 $x_{c3} = 0.435$; $V_3 = 858$ Å^3 $x_{c4} = 1.0$	 $x_{c3} = 0.44$ $x_{c4} = 1.0$		

[a] Degree of deuteration $\eta = 0.902$. [b] According to Gershfield (1978).

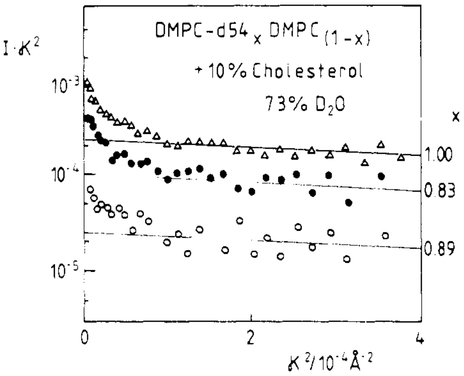

FIGURE 1: Typical Kratky–Porod plots of liposomes of DMPC–cholesterol mixtures with varying molar fraction, x, of deuterated lecithin (DMPC-d_{54}) to protonated DMPC: $x = 1.0$ (▲); $x = 0.89$ (○); $x = 0.83$ (●). The D_2O content was 73% and the temperature 7 °C.

viously (Knoll et al., 1985a) I_0 is now expressed in terms of the molar fraction x

$$I_0 \propto \frac{x_2 - x_c}{x_2 - x_1} \times \left(\frac{x_1 b_C + (1 - x_1) x b_D{}^d + (1 - x_1)(1 - x) b_D{}^P}{V_1} - \rho_s \right)^2 + \frac{x_c - x_1}{x_2 - x_1} \left(\frac{x_2 b_C + (1 - x_2) x b_D{}^d + (1 - x_2)(1 - x) b_D{}^P}{V_2} - \rho_s \right)^2 \quad (3)$$

b_C, $b_D{}^P$, and $b_D{}^d$ are the scattering lengths of the cholesterol and the protonated and the deuterated DMPC, respectively. V_1 and V_2 are the molar volumes of phase 1 and 2, respectively.

The scattering lengths of b_C and $b_D{}^P$ are $b_C = 1.325 \times 10^{-12}$ cm and $b_D{}^P = 3.101 \times 10^{-12}$ cm. The value $b_D{}^d$ for the deuterated DMPC-d_{54} has been measured separately since it depends on the degree of deuteration of this compound (Knoll et al., 1985a). We obtained $b_D{}^d = 53.83 \times 10^{-12}$ cm.

The molar volumes V_1 and V_2 are also measured by mass densitometry (Schmidt & Knoll, 1985). The scattering length densities and molar volumes are summarized in Table I. The phase boundaries x_1 and x_2 can now be determined by fitting the theoretical curve of eq 3 to the experimental I_0 vs. x curves. One has to apply this procedure to two mixtures of different initial cholesterol content x_c in order to determine x_1 and x_2 unambiguously.

RESULTS

Figure 1 shows typical Kratky–Porod plots of a DMPC–cholesterol mixture containing 10 mol % of the latter. Curves at various fractions, x, of the deuterated lecithin are shown. Clearly, the Kratky–Porod law is fulfilled to very low-scattering vectors: $\kappa > 10^{-2}$ Å^{-1}. The zero intensity I_0 is obtained by extrapolation of the straight lines to $\kappa = 0$. I_0 decreases with the molar fraction, x, of the deuterated DMPC-d_{54} until the bilayer and the aqueous phase become contrast matched. Simultaneously, the relative error of the scattering increases, which shows the limit of resolution of the technique.

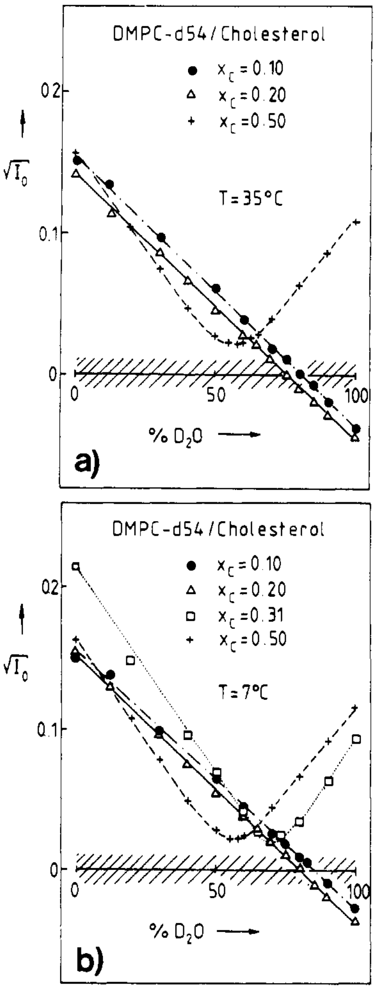

FIGURE 2: Result of the conventional contrast variation experiments. (a) Plots of $I_0{}^{1/2}$ vs. percentage of D_2O for cholesterol contents of $x_c = 0.10$ (●), $x_c = 0.20$ (▲), and $x_c = 0.50$ (+). The dashed area above and below the abscissa denotes the limit of sensitivity of the method. $T = 35$ °C. (b) Same type of experiment performed at 7 °C for cholesterol contents at $x_c = 0.10$ (●), $x_c = 0.20$ (▲); $x_c = 0.31$ (□), and $x_c = 0.50$ (+).

Figure 2 shows the results of the conventional contrast variation experiment of the DMPC-d_{54}–cholesterol mixture at 35 °C well above the chain melting (Figure 2a) and below the $P_{\beta'} \leftrightarrow L_{\beta'}$ pretransition (Figure 2b) of the pure lecithin. Within experimental error, contrast matching is achieved for $x_c = 0.10$ and $x_c = 0.20$, both in the $L_{\beta'}$ and in the L_α phase of the lecithin, while the 1:1 mixture is certainly not maskable. Also the mixture with $x_c = 0.31$ is certainly heterogeneous at 7 °C. The apparent maskability at $x_c = 0.1$ and $x_c = 0.2$ at 7 °C is surprising, since it would contradict the experimental evidence for lateral phase separation between 10 and 20 mol

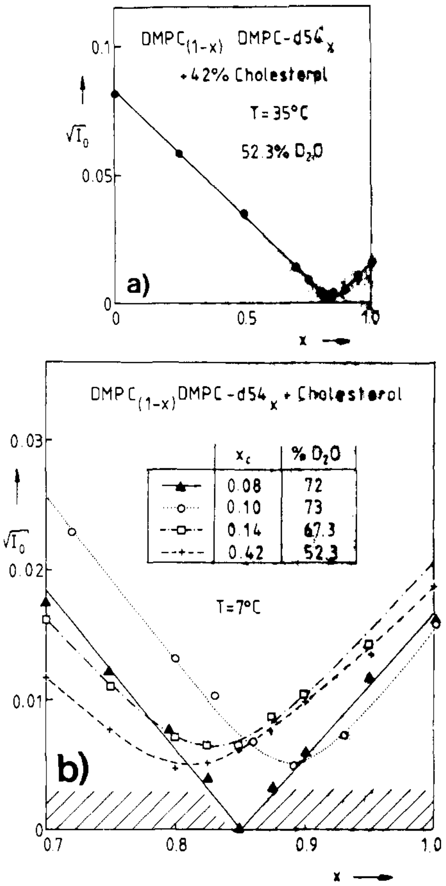

FIGURE 3: Inverse contrast variation (ICV) experiments of DMPC–cholesterol mixtures of various composition at various D_2O content. $I_0^{1/2}$ is plotted as a function of the molar fraction of DMPC-d_{54}. (a) $I_0^{1/2}$ vs. x plot for the whole range of possible DMPC-d_{54} molar ratios for $x_c = 0.42$ and for the L_α phase of DMPC-d_{54}. (b) $I_0^{1/2}$ vs. x plots in the region of low contrast for $x_c = 0.08$ (▲), $x_c = 0.10$ (○), $x_c = 0.14$ (□), and $x_c = 0.42$ (+). All curves are taken at 7 °C ($L_{\beta'}$ phase of DMPC-d_{54}). The dashed horizontal band indicates again the lower limit of measurability of $I_0^{1/2}$. Note that the ordinate is expanded by a factor of 10 as compared to Figure 2.

% of cholesterol reported in the literature (cf. Melchior et al., 1980; Albrecht et al., 1981). The suspicion that this contradiction is due to the low sensitivity of the method (cf. Figure 2a) led us to introduce the inverse contrast variation (ICV) technique.

The essential results of this technique are presented in Figure 3. In Figure 3a $I_0^{1/2}$ is plotted over the whole range of possible molar fractions, x, of the deuterated lecithin at a constant solvent scattering density $\rho_s = 3.05 \times 10^{10}$ cm^{-2} ($\approx$52.3% D_2O) for a mixture containing 58 mol % lecithin and 42 mol % cholesterol. Figure 3b shows $I_0^{1/2}$ vs. x plots for mixtures of various composition and D_2O content at enlarged scale of the abscissa ($0.7 < x < 1.0$) and of the ordinate ($0 < I_0^{1/2} < 0.03$). Values of $I_0^{1/2}$ as small as $I_0^{1/2} = 0.003$ may be measured; that is, the ICV is by about a factor of 5 more sensitive than the conventional technique (cf. Figure 2a).

According to Figure 3a the $I_0^{1/2}$ vs. x plot yields nearly a straight line for x values far from the minimum. For that reason we consider only the ICV curve in the neighborhood of the minimum. With this improved technique it is now clearly demonstrated that the mixture containing $x = 0.1$ of cholesterol exhibits a slight heterogeneity at 7 °C. The same holds for $x_c = 0.14$ while a homogeneous solution is formed at $x_c = 0.08$. Another important finding is that at $x_c = 0.42$, again a slightly heterogeneous mixture is observed both in the L_α and in the $L_{\beta'}$ phase.

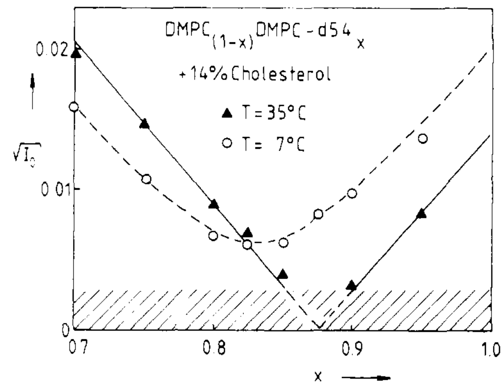

FIGURE 4: Comparison of the ICV curves of mixture containing 14 mol % cholesterol in the L_α (▲) and the $L_{\beta'}$ phase (○) of DMPC-d_{54}, respectively.

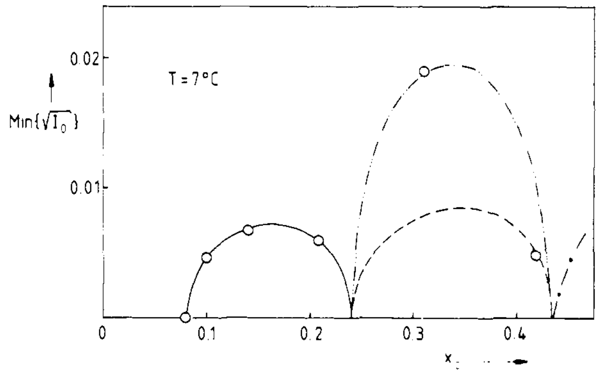

FIGURE 5: Plot of the minimum value of $I_0^{1/2}$ as obtained from the $I_0^{1/2}$ vs. composition curves of Figures 2–4. The lines are the theoretically expected behavior. The full line represents the minimum of $I_0^{1/2}$ of an ICV experiment calculated according to eq 3 for different x_c ($x_{c1} < x_c < x_{c2}$) with $x_{c1} = 0.08$ and $x_{c2} = 0.24$ as phase boundaries. The dashed line shows the equivalent result for $x_{c2} < x_c < x_{c3}$ with $x_{c2} = 0.24$ and $x_{c3} = 0.435$ as phase boundaries. The dashed–dotted line is the expected result of a classical contrast variation experiment according to eq 2 with $\bar{\rho}_1$ = average scattering length density of the phase with $x_{c2} = 0.24$ and $\bar{\rho}_2$ that of the phase with $x_{c3} = 0.435$. The line for $x_c > 0.435$ (···) indicates schematically that the phase with $x = 0.435$ which is supposedly the solubility limit of cholesterol in DMPC coexists with pure cholesterol organized as small precipitated crystallites.

In order to decide whether the heterogeneous lipid distribution is due to lateral phase separation or to a decomposition of the mixture in vesicles of different composition (heterogeneous phase separation), it is helpful to perform contrast variation experiments of the same sample at different temperatures. An example is given in Figure 4. Obviously, the mixture with $x_c = 0.14$ is homogeneous if DMPC is fluid but heterogeneous if it is in the $L_{\beta'}$ phase, and it thus exhibits lateral phase separation.

The next aim is to determine the phase boundaries by fitting the theoretical $I_0^{1/2}$ vs. x curve of eq 2 to the experimental data. As a first step one has to guess the approximate position of the phase boundaries: For that purpose it is useful to compare the depths of the minima of the contrast variation curves as obtained for the different cholesterol contents. These minimum values of $I_0^{1/2}$ are plotted in Figure 5 as a function of x_c for the $L_{\beta'}$ phase of DMPC. Phase boundaries are strongly suggested at $x_{c1} = 0.08$ and $x_{c3} = 0.435$, and there is some indication for a third boundary at $x_{c2} = 0.24$ and a fourth one at $x_c \approx 1.0$. It is indeed found that the experimental curves can only be fitted by assuming that there are four phase boundaries at $T = 7$ °C. Figure 6 shows the results of the fitting procedure. First, the phase boundaries x_{c1} and x_{c2} were

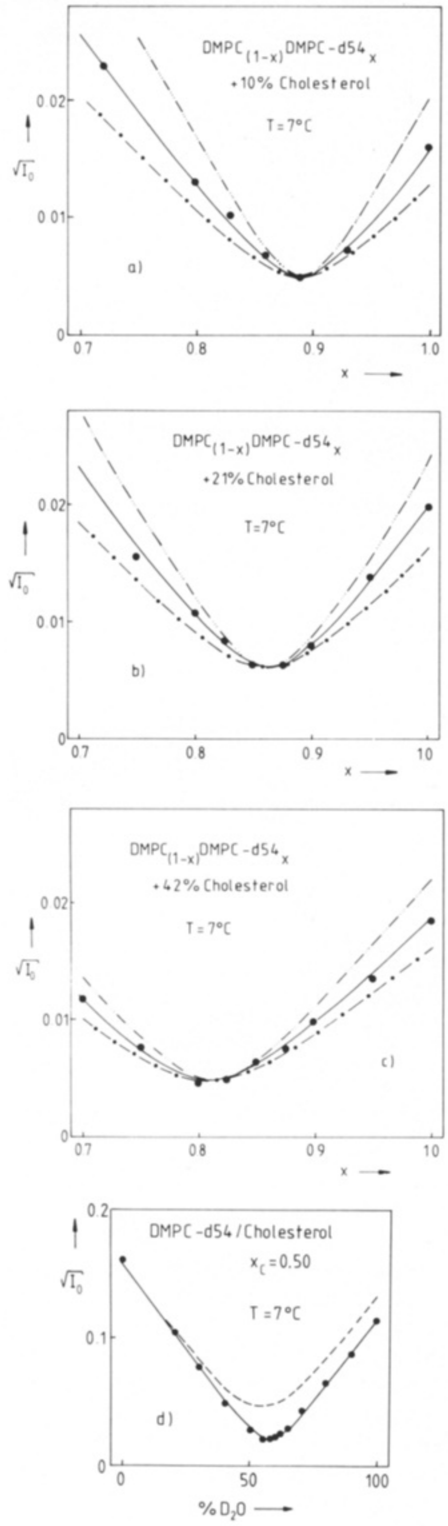

FIGURE 6: Determination of phase boundaries by fitting experimental $I_0^{1/2}$ vs. x plots with theoretical curves according to eq 3 (a–c) and $I_0^{1/2}$ vs. percent D$_2$O plots according to eq 2 (d). (a) ICV data with $x_c = 0.10$ (●). The theoretical lines are calculated with $x_{c2} = 0.24$ and $x_{c1} = 0.08$ (—), $x_{c1} = 0.09$ (-·-·-·), and $x_{c1} = 0.07$ (---), respectively. (b) ICV data with $x_c = 0.21$ (●). Theoretical lines calculated with $x_{c1} = 0.08$ and $x_{c2} = 0.24$ (—), $x_{c2} = 0.23$ (-·-·-·), and $x_{c2} = 0.25$ (---), respectively. (c) ICV data with $x_c = 0.42$ (●). Theoretical lines calculated with $x_{c2} = 0.24$ and $x_{c3} = 0.435$ (—), $x_{c3} = 0.43$ (-·-·-·), and $x_{c3} = 0.44$ (---), respectively. (d) Fitting of data of conventional contrast variation experiment with $x_c = 0.50$ (●). The dashed curve was calculated with $x_{c3} = 0.435$ and $x_{c4} = 1.0$. The full line was obtained by assuming that 6 mol % cholesterol was lost due to heterogeneous phase separation, i.e., $x_c = 0.44$ instead of $x_c = 0.50$.

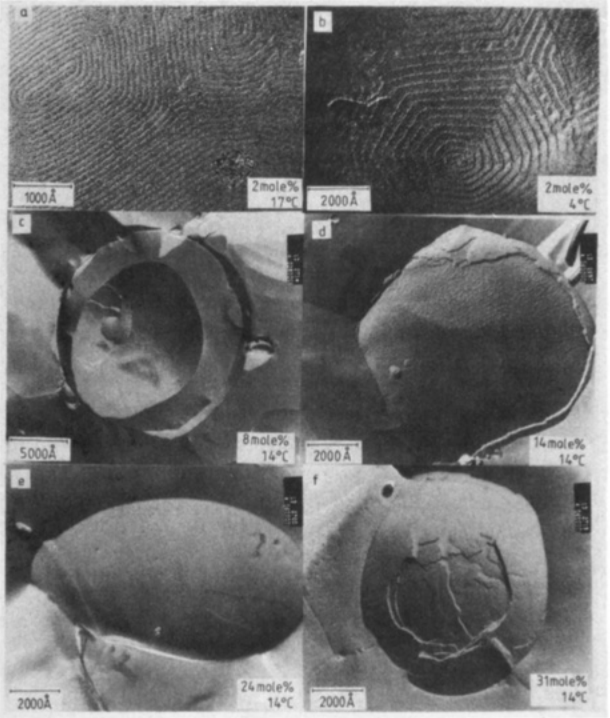

FIGURE 7: Freeze–fracture electron micrographs of DMPC–cholesterol mixed vesicles of various composition indicated in the micrograph. For 2 mol % cholesterol the textures obtained upon freezing the preparation from a temperature between T_m and T_p and below T_p, respectively, are presented. For the other compositions the texture is the same for the two situations, and micrographs are only shown for preparations frozen from 14 °C.

determined by fitting the data for $x_c = 0.1$, $x_c = 0.14$, and $x_c = 0.21$ (cf. Figure 6a,b) while x_{c3} was obtained by calculating the ICV curves for $x_c = 0.42$ (Figure 6c). It is seen that the fitting procedure is very sensitive in the case of the ICV method which enables one to determine the phase boundaries to an accuracy of ±0.5%. In the case of the conventional technique the accuracy is much worse (±2%).

The case of the 1:1 mixture deserves a separate consideration. It clearly exhibits phase separation both in the L$_\alpha$ and in the L$_{\beta'}$ phase. Electron microscopic observations provide evidence that cholesterol precipitates as small crystals at very high concentrations (Fischer, 1984) so that $x_{c4} = 1$ is a phase boundary at all temperatures. The contrast variation curves can, however, not be fitted sufficiently with $x_{c3} = 0.435$ and $x_{c4} = 1.0$ (cf. Figure 6d, dashed line). Good fit is observed, however, if one assumes that part of the cholesterol has been lost during the preparation. This provides evidence that $x_{c3} = 0.435$ is the limit of solubility of cholesterol in DMPC.

The DMPC-d_{54}/cholesterol mixed vesicles have also been studied by freeze–fracture electron microscopy. Some results obtained for cholesterol concentrations at and between the phase boundaries, x_{c1}, x_{c2}, and x_{c3}, are shown in Figure 7. For $x_c = 0.02$, micrographs of a sample cooled from a temperature between (17 °C; Figure 7a) the main-transition and the pretransition and below the latter (4 °C; Figure 7b) are shown. The surface textures are clearly distinguished with respect to both the repeat distance of the ripples (which is $d = 140$ Å at 17 °C and $d = 250$ Å at 4 °C) and the surface profile. The latter difference has been discussed previously (Sackmann et al., 1980). The above differences in the texture are only observed up to $x_c = 0.05$ while it is identical at $T < T_p$ and $T_p < T < T_m$ for higher cholesterol concentrations. This finding corresponds well with the observation that the pretransition is abolished at $x_c \geq 0.06$ (Estep et al., 1978). At

$x_c = 0.08$ one observes still a regular ripple texture (Figure 7c) with a repeat distance ($d = 140$ Å) that agrees well with that observed for the 2% mixture or for pure DMPC for which $d = 140$ Å. (Sackmann et al., 1980). A closer inspection shows, however, that the distance fluctuates more strongly for $x_c = 0.08$ ($\delta_d \approx \pm 30$ Å) than for $x_c = 0.02$ or for pure DMPC ($\delta_d \approx \pm 10$ Å). If the cholesterol content is increased above x_{c1}, the ripple texture is completely distorted (cf. Figure 7d); that is, the vesicle surface exhibits elongated smooth patches separated by damlike protrusions. The density of the latter decreases with increasing cholesterol content, and a repeat distance cannot be defined anymore. At the phase boundary x_{c2} ($x_{c2} = 0.24$), finally all vesicles inspected in the replica (about 20) exhibit a completely smooth surface as shown in the example of Figure 7e. A smooth surface texture is also observed if the cholesterol content is increased further to $x_c = 0.31$ (Figure 7f) and $x_c = x_{c3} = 0.43$. The only difference as compared to the 24% mixture is that the liposomes appear to be more strongly deformed. Moreover, the bilayers exhibit an increasing tendency toward aggregation into multibilayers with increasing cholesterol content.

Discussion

With the introduction of the inverse contrast variation technique, the sensitivity of the small-angle neutron scattering for the determination of phase separation in membranes is drastically improved. Per contrast variation 10–20 mg of lipid is needed, and the total measuring time is about 2 h at a high flux reactor. At present SANS is still an expensive technique, and it can therefore only be used to determine some of the essential points of the phase diagram.

For temperatures well above the chain melting transition of DMPC we clearly demonstrated miscibility up to 14 mol % cholesterol. Moreover, our experiments lead to the conclusion that at $x_c \approx 0.5$ the mixture decomposes into a saturated solution of cholesterol in DMPC and crystals of cholesterol. Evidence for this conclusion is provided by the finding that the minimum $I_0^{1/2}$ is equally pronounced at 35 and 7 °C. At $x_c = 0.42$ one observes only a very weak residual nonmaskability which suggests that this corresponds to the limit of solubility of cholesterol in DMPC. It is interesting to note that the many biological membranes such as the plasma membrane of erythrocytes or myelin contain about 50% of cholesterol which would well be attributed to the fact that these membranes are saturated with cholesterol.

In the case of the $L_{\beta'}$ phase we could clearly determine three phase boundaries at $x_{c1} = 0.08$, $x_{c2} = 0.24$, and $x_{c3} = 0.435$ and obtained evidence for a fourth, x_{c4}, close to 1.0. The phase boundary at x_{c2} has actually been observed previously by several groups by using different spectroscopic methods such as photobleaching (Owicki & McConnell, 1980), fluorescence polarization experiments (Lentz et al., 1980), and spin-label studies (Recktenwald & McConnell, 1981). Clear evidence for this phase boundary comes also from microcalorimetric studies of Mabrey et al. (1978) and Estep et al. (1978) or from densitometric measurements of Melchior et al. (1980) although these authors did not discuss their data strictly in terms of phase separation. In both types of measurements one observes a superposition of a sharp and a broad band. The latter increases in intensity on the cost of the first one which vanishes at $x_c \approx 0.2$. A phase boundary at $x_{c2} = 0.2$ has clearly been observed for mixed monolayers of DPPC and cholesterol (Albrecht et al., 1981).

Our experiments do not provide any evidence for phase separation above the gel states of DMPC at $x_c \leq 0.2$ and are thus at variance with the conclusion of Recktenwald & McConnell (1981) based on their spectroscopic studies. In this context it should be pointed out that the molecular motions such as lateral diffusion (Galla et al., 1979) or rotational motions and most likely also TEMPO binding depends on the packing density of the lipid molecules. A nonideal behavior of the molar areas (or volumes) of a mixture may thus well lead to breaks in the TEMPO partitioning or molecular mobilities which could then be erroneously interpreted in terms of phase boundaries.

A problem arises by our finding that two coexistence regions meet at $x_{c3} = 0.24$ which seems to be in contrast with the phase rule. Since we think that our data provide clear evidence for the adjoining coexistence regions, we are led to the conclusion that the phase boundary x_{c2} corresponds to a stoichiometric 7:1 mixture of DMPC and cholesterol. As is well-known that the appearance of a stoichiometric mixture is equivalent to the introduction of a new component so that two coexistence regions may meet at such a mixture. There have been numerous attempts to interpret the experimental data concerning lecithin/cholesterol mixtures in terms of complex formation. It has been shown that 7:1 and 3:1 mixtures allow for a particularly dense packing (Cadenhead & Müller-Landau, 1984). The concept of phase separation and complex formation may thus be reconciled.

The freeze–fracture micrographs of Figure 7 are representative examples. It has been verified, however, by inspection of some 20 vesicles for each case that at a given concentration the overwhelming majority of vesicdles (about 95%) show the same type of texture.

The freeze–fracture results for $T < T_m$ correspond well with those of the SANS experiments:

(1) At cholesterol contents up to 8 mol % a regular ripple structure with a constant repeat distance equal to that characteristic for pure DMPC is found, which verifies our above conclusion that a solution of cholesterol in DMPC is formed at $x_c \leq 0.08$. According to the calorimetric studies [e.g., see Mabrey et al. (1978)] the solid to fluid phase transition of this solid solution at T_m is decreased by about 1 °C between $x_c = 0$ and $x_c = 0.08$.

(2) Within the phase boundaries x_{c1} and x_{c2} all vesicles exhibit an irregular texture consisting of elongated smooth patches separated by damlike protrusions. The latter phase corresponds to the saturated solid solution of cholesterol in DMPC, and its protrusion in the third dimension provides clear evidence that the hydrocarbon chains are still tilted (Sackmann et al., 1980). The former phase is not tilted.

(3) At $x_c = 0.24$, all vesicles exhibit a completely smooth surface. This shows that a homogeneous phase is formed in agreement with SANS experiments.

Between 24 and 43% cholesterol the freeze–fracture technique can no longer give information concerning lateral phase separation because the surface texture of the vesicles is essentially smooth. Some evidence for phase separation is provided by the finding that the vesicles tend to fold during the freezing process (cf. Figure 7f).

(4) Above $x_{c3} = 0.43$, one observes small particles in the freeze–fracture micrographs which could be due to cholesterol precipitates. Small crystallites of cholesterol are indeed found in electron diffraction studies of dried vesicle suspension at $x_c = 0.5$ (Fischer, 1984).

In contrast to Copeland & McConnell (1980) we do not find a variation of the ripple repeat distance, with the cholesterol concentration at $x_c \leq x_{c1} = 0.08$. Within experimental error it is $d = 140 \pm 20$ Å; that is, the ripple texture corresponds to the $\Lambda/2$ phase defined previously (Sackmann et al., 1980).

According to a previously proposed model of the ripple phase based on the concept of a spontaneous monolayer curvature (Gebhardt et al., 1977), the repeat distance should depend only weakly on the bilayer bending elastic stiffness, K_{11} ($d \propto K_{11}^{1/5}$). A change in K_{11} by incorporation of cholesterol in DMPC should thus leave d essentially unchanged. The cholesterol could also accumulate preferentially at the minma and maxima of the ripples which exhibit a high density of chain defects (Rüppel & Sackmann, 1983).

Above $x_c = 0.08$ a ripple repeat distance cannot be defined anymore. The appearance of the distorted ripple texture depends critically on the freezing time. At slow cooling rates it becomes more regular. In terms of the theory of spinodal decomposition this finding can be explained as a coarsening process (Sackmann et al., 1980). The regular texture reported by Copeland & McConnell (1980) and Lentz et al. (1980) could be due to this effect.

Finally, the question arises whether DMPC-d_{54}–DMPC–cholesterol can be considered as a binary mixture. In a previous study we showed that the mixture of deuterated and protonated DMPC behaves as a completely ideal system, and it is therefore well justified to consider the DMPC-d_{54}–DMPC mixture as a single component for our purpose (Knoll et al., 1985a). The protonated and deuterated lipids behave certainly different with respect to chain dynamics or the kinetics of the phase transitions but not with respect to their equilibrium properties.

ACKNOWLEDGMENTS

The freeze–fracture experiments and the drawing were done by C. Fahn to whom we are most grateful.

Registry No. DMPC, 18194-24-6; cholesterol, 57-88-5.

REFERENCES

Albrecht, O., Gruler, H., & Sackmann, E. (1981) *J. Colloid Interface Sci. 79*, 319–338.

Cadenhead, D. A., & Müller-Landau, F. (1984) *Can. J. Biochem. Cell Biol. 62*, 732–737.

Copeland, B. R., & McConnell, H. M. (1980) *Biochim. Biophys. Acta 599*, 95–109.

Estep, T. N., Mountcastle, D. B., Biltonen, R. L., & Thomson, T. E. (1978) *Biochemistry 17*, 1984–1989.

Fischer, A. (1984) Ph.D. Thesis, München.

Galla, H. J., Hartmann, W., Theilen, U., & Sackmann, E. (1979) *J. Membr. Biol. 48*, 215–236.

Gebhardt, C., Gruler, H., & Sackmann, E. (1977) *Z. Naturf., C: Biosci. 32C*, 581–596.

Gershfield, N. L. (1978) *Biophys. J. 22*, 469–488.

Hui, S. W., & He, N.-B. (1983) *Biochemistry 22*, 1159–1164.

Knoll, W., Haas, J., Stuhrmann, H. B., Füldner, H.-H., Vogel, H., & Sackmann, E. (1981a) *J. Appl. Crystallogr. 14*, 191–202.

Knoll, W., Ibel, K., & Sackmann, E. (1981b) *Biochemistry 20*, 6379–6383.

Knoll, W., Schmidt, G., & Ibel, K. (1985a) *J. Appl. Crystallogr. 18*, 65–70.

Knoll, W., Schmidt, G., & Ibel, K. (1985b) *J. Appl. Crystallogr. 18*, 61–64.

Lentz, B. R., Barrow, D. A., & Hoechli, M. (1980) *Biochemistry 19*, 1943–1954.

Mabrey, S., Mateo, P. L., & Sturtevant, J. M. (1978) *Biochemistry 17*, 2464–2468.

Melchior, D. L., Scavitto, F. J., & Steim, J. M. (1980) *Biochemistry 19*, 4828–4834.

Owicki, J. C., & McConnell H. M. (1980) *Biophys. J. 30*, 383–397.

Pink, D., & Chapman, D. (1979) *Proc. Natl. Acad. Sci. U.S.A. 76*, 1542–1546.

Recktenwald, D., & McConnell, H. M. (1981) *Biochemistry 20*, 4505–4510.

Rüppel, D., & Sackmann, E. (1983) *J. Phys. (Les Ulis, Fr.) 44*, 1025–1034.

Sackmann, E., Rüppel, D., & Gebhardt, C. (1980) *Springer Series Chem. Phys. 11*, 309–326.

Schmidt, G., & Knoll, W. (1985) *Ber. Bunsenges. Phys. Chem. 89*, 36–43.